# The Golgi apparatus in the endomembrane-rich gastric parietal cells exist as functional stable mini-stacks dispersed throughout the cytoplasm

**Priscilla A. Gunn\*, Briony L. Gliddon\*[1], Sarah L. Londrigan†[2], Andrew M. Lew†, Ian R. van Driel\* and Paul A. Gleeson\*[3]**

\*Department of Biochemistry and Molecular Biology and Bio21 Molecular Science and Biotechnology Institute, The University of Melbourne, Victoria 3010, Australia, and †The Walter and Eliza Hall Institute of Medical Research, Parkville 3052, Victoria 3010, Australia

*Background information.* Acid-secreting gastric parietal cells are polarized epithelial cells that harbour highly abundant and specialized, $H^+,K^+$ ATPase-containing, tubulovesicular membranes in the apical cytoplasm. The Golgi apparatus has been implicated in the biogenesis of the tubulovesicular membranes; however, an unanswered question is how a typical Golgi organization could regulate normal membrane transport within the membrane-dense cytoplasm of parietal cells.

*Results.* Here, we demonstrate that the Golgi apparatus of parietal cells is not the typical juxta-nuclear ribbon of stacks, but rather individual Golgi units are scattered throughout the cytoplasm. The Golgi membrane structures labelled with markers of both *cis*- and *trans*-Golgi membrane, indicating the presence of intact Golgi stacks. The parietal cell Golgi stacks were closely aligned with the microtubule network and were shown to participate in both anterograde and retrograde transport pathways. Dispersed Golgi stacks were also observed in parietal cells from $H^+,K^+$ ATPase-deficient mice that lack tubulovesicular membranes.

*Conclusions.* These results indicate that the unusual organization of individual Golgi stacks dispersed throughout the cytoplasm of these terminally differentiated cells is likely to be a developmentally regulated event.

## Introduction

The Golgi apparatus is an integral component of the secretory and retrograde transport pathways in mammalian cells. In most mammalian interphase cells, the Golgi exists as a juxta-nuclear ribbon, composed of a network of membrane stacks, interlinked by tubular membrane connections (De Matteis et al., 2008). The individual stacks are units of 4–8 flattened, cisternal membrane structures (Short et al., 2005). Golgi-derived microtubules have been proposed to draw individual stacks together, a process regulated by the microtubule-binding proteins CLASPs (CLIP-associated proteins), to promote the formation of a continuous ribbon (Efimov et al., 2007; Miller et al., 2009). In addition, in non-polarized cells, the radial microtubule array positions the Golgi adjacent to the MTOC (microtubule-organizing centre) close to the nucleus (Rogalski et al., 1984; Thyberg and Moskalewski, 1985; Rios and Borens, 2003). On the other hand, in polarized cells, in which microtubules
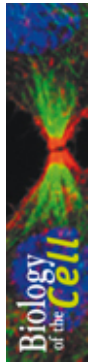
are typically aligned along the apical–basal axis with minus ends predominantly at the apical pole (Li and Gundersen, 2008), and the Golgi typically forms a ribbon-like convoluted structure located in the apical region above the nucleus (Bacallao et al., 1989).

The organization of the Golgi apparatus is highly dynamic. Regulated fragmentation of the Golgi occurs during mitosis (Nelson, 2000; Colanzi et al., 2003) and repositioning of the Golgi can occur during a number of processes, including directed secretion and pathogen invasion (Kupfer et al., 1983; Yadav et al., 2009). For example, when *Chlamydia trachomatis* invades a mammalian cell, a membrane-bound niche called an inclusion is established, and the host Golgi is fragmented so that the remnant Golgi membrane can be aligned around the inclusion (Heuer et al., 2009). Hence there is considerable plasticity in the arrangement of the Golgi stacks to accommodate important cellular events. Despite this, investigations into the dynamics of the Golgi have been restricted to a few cell types.

Parietal cells are terminally differentiated, polarized epithelial cells that are responsible for the acidification of the stomach (Forte et al., 1977; Yao and Forte, 2003). Parietal cells express the gastric $H^+,K^+$ ATPase, which catalyses the transfer of $H^+$ ions across the apical membrane of the cell and into the lumen of the stomach in exchange for $K^+$ ions (van Driel and Callaghan, 1995; Shin et al., 2009). Control of acid secretion is achieved, in part, by shuttling the membrane-bound $H^+,K^+$ ATPase between two specialized membrane compartments in parietal cells: invaginations of the apical membrane which are called SC (secretory canaliculi) and an extended membrane compartment in the cytoplasm which is called the TVE (tubulovesicular element) (Yao and Forte, 2003; Geibel and Wagner, 2006; Forte and Zhu, 2010). A unique feature of gastric epithelial cells is the great abundance of these $H^+,K^+$ ATPase-containing SC and TVE membranes. Early observations by EM (electron microscopy) showed the presence of abundant Golgi membranes in developing parietal cells (Hayward, 1967; Forte et al., 1969), prompting the suggestion that the Golgi is the site of production and synthesis of the $H^+,K^+$ ATPase-rich membrane (Forte et al., 1969).

Very little is known about the organization of the Golgi apparatus in mature parietal cells. In contrast with developing parietal cells, the Golgi has been considered to be small and relatively inconspicuous in fully developed parietal cells (Forte et al., 1969; Ito, 1987; Sawaguchi et al., 2002). The very high density of the specialized SC and TVE membranes in the apical cytoplasm of mature parietal cells is likely to pose a challenge to the convention of a juxta-nuclear-localized Golgi ribbon network to regulate the normal membrane transport in the secretory and endocytic pathways. Based on the terminal sequences of the N-glycans of the $H^+,K^+$ ATPase $\beta$-subunit, there is indirect evidence that $H^+,K^+$ ATPase may recycle via the TGN (*trans*-Golgi network) (Nguyen et al., 2004); however, how a retrograde transport pathway for such recycling would occur in this cell type is not clear. The aim of this work was to define the localization and transport functions of the Golgi in parietal cells. We show that the Golgi is not present as a ribbon of membrane in the juxta-nuclear region in these cells, but exists as individual units of Golgi membrane scattered throughout the cytoplasm, an unusual organization for mammalian cells. These units of Golgi membrane were demonstrated to be functional Golgi stacks.

## Results

### The Golgi apparatus is present as dispersed stacks in mouse parietal cells

To analyse the organization of the Golgi apparatus in gastric parietal cells initially, we characterized cultured gastric cells. Gastric cells were stained for actin, the *cis*-Golgi marker GM130 (*cis*-Golgi matrix protein of 130 kDa) and DNA. Non-parietal cells in the population, identified by an abundant sub-plasma membrane actin staining, showed a juxta-nuclear staining pattern for GM130, typical for the Golgi ribbon of mammalian cells. In contrast, parietal cells that were identified by the presence of actin-rich intracellular SC vacuoles (Figure 1B), had a strikingly different GM130 staining pattern. GM130 was located on punctate fragments scattered throughout the cytoplasm of the parietal cell. The majority of the GM130-positive structures were not close to the nucleus but rather were scattered throughout the cell periphery. The GM130 staining pattern shown in Figure 1(B) was similar in all parietal cells (>100) examined.

To define the nature of the dispersed GM130-positive structures in parietal cells more precisely, we

**Figure 1 | The Golgi staining pattern of cultured gastric cells**

Gastric cell populations were isolated from the stomachs of wild-type mice (fasted) and cultured for 24 h in gland culture medium containing ranitidine. Cells were fixed in 1% formaldehyde, permeabilized and stained with TRITC-conjugated phalloidin, DAPI and mouse anti-GM130 (*cis*-Golgi marker) antibodies followed by FITC-conjugated anti-mouse IgG. (**A**) Non-parietal gastric cell and (**B**) parietal cell. The broken white line denotes the boundary of an individual cell. Scale bars represent 10 $\mu$m.
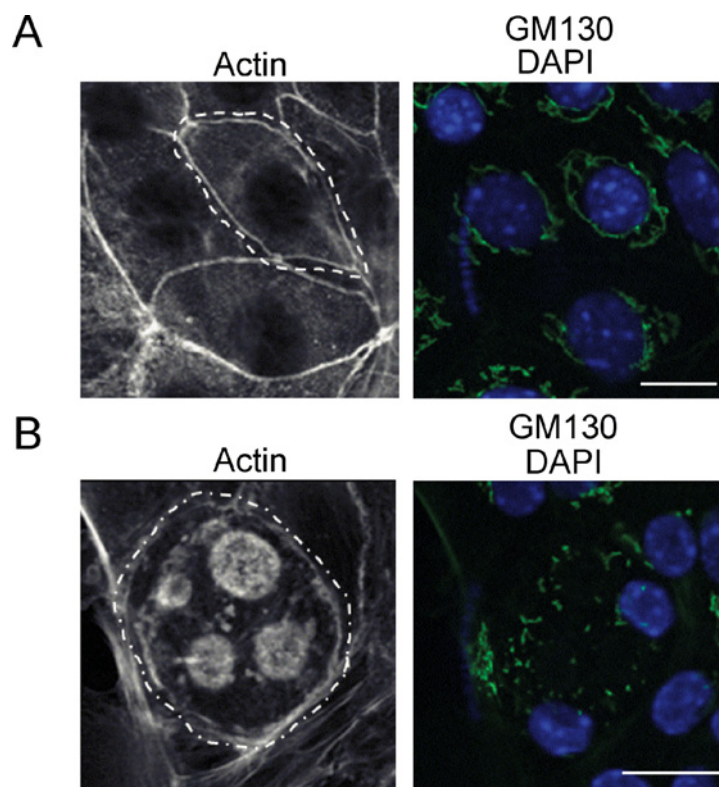


employed additional Golgi markers and examined the relationship between *cis*- and *trans*-cisternae in the Golgi fragments. A population of cultured gastric cells was stained simultaneously with antibodies against the *cis*-Golgi marker GM130 and the TGN marker syntaxin 16 (Figure 2A). The majority of Golgi units scattered throughout the cytoplasm contained markers of both *cis*- and *trans*-cisternae, which implied that the Golgi units were likely to represent intact Golgi stacks. To better define the spatial distribution of Golgi structures in whole parietal cells, a *z*-series of labelled parietal cells were captured by confocal microscopy and a 3D image reconstructed (Supplementary Movie 1 available at http://www.biolcell.org/boc/103/boc1030559add.htm). The reconstructed *z*-series of stained parietal cells demonstrated that the Golgi punctate structures were not interconnected but existed as distinct entities.

To attain an estimate of the proportion of Golgi units which were labelled with markers of both *cis*- and *trans*-Golgi, we analysed a total of 191 individual Golgi units in three different cells, with the Golgi units identified as GM130-positive and/or GCC185 (Golgi coiled-coil protein of 185 kDa)-positive. Of the 191 Golgi units, 139 (73%) were co-labelled with GM130 and GCC185, with the remaining 52 units (27%) singly labelled with either marker. Another population of cultured gastric cells was stained with antibodies against two markers of the TGN, GCC185 and p230 (Figure 2B). GCC185 and p230 are Golgins of the TGN which are thought to be associated with distinct domains of this Golgi compartment (Chia and Gleeson, 2011). The majority of Golgi structures (94/101: 93.1%) co-labelled with both markers (Figure 2B), again indicating that the membrane

**Figure 2 | Location of *cis*- and *trans*-Golgi markers in cultured parietal cells and gastric glands**

(**A**, **B**) Gastric cell populations were cultured for 24 h in gland culture medium containing ranitidine, then fixed in 1% formaldehyde, permeabilized and stained with either (**A**) TRITC-conjugated phalloidin, mouse anti-GM130 (*cis*-Golgi marker) antibodies followed by FITC-conjugated anti-mouse IgG and rabbit anti-syntaxin 16 (TGN marker) antibodies followed by Alexa Fluor® 647-conjugated to anti-rabbit IgG or (**B**) mouse anti-HKα antibodies followed by FITC-conjugated anti-mouse IgG, rabbit anti-GCC185 (TGN marker) antibodies followed by Alexa Fluor® 647-conjugated anti-rabbit IgG (pseudo-coloured green) and human anti-p230 (TGN marker) antibodies followed by Alexa Fluor® 594-conjugated to anti-human IgG. (**C**) Gastric glands were isolated from the stomachs of wild-type mice (fasted) and fixed in 4% PFA, permeabilized and stained with TRITC-conjugated phalloidin, mouse anti-GM130 antibodies followed by FITC-conjugated anti-mouse IgG and rabbit anti-syntaxin16 (TGN marker) antibodies followed by Alexa Fluor® 647-conjugated to anti-rabbit IgG. Scale bars represent 10 μm.
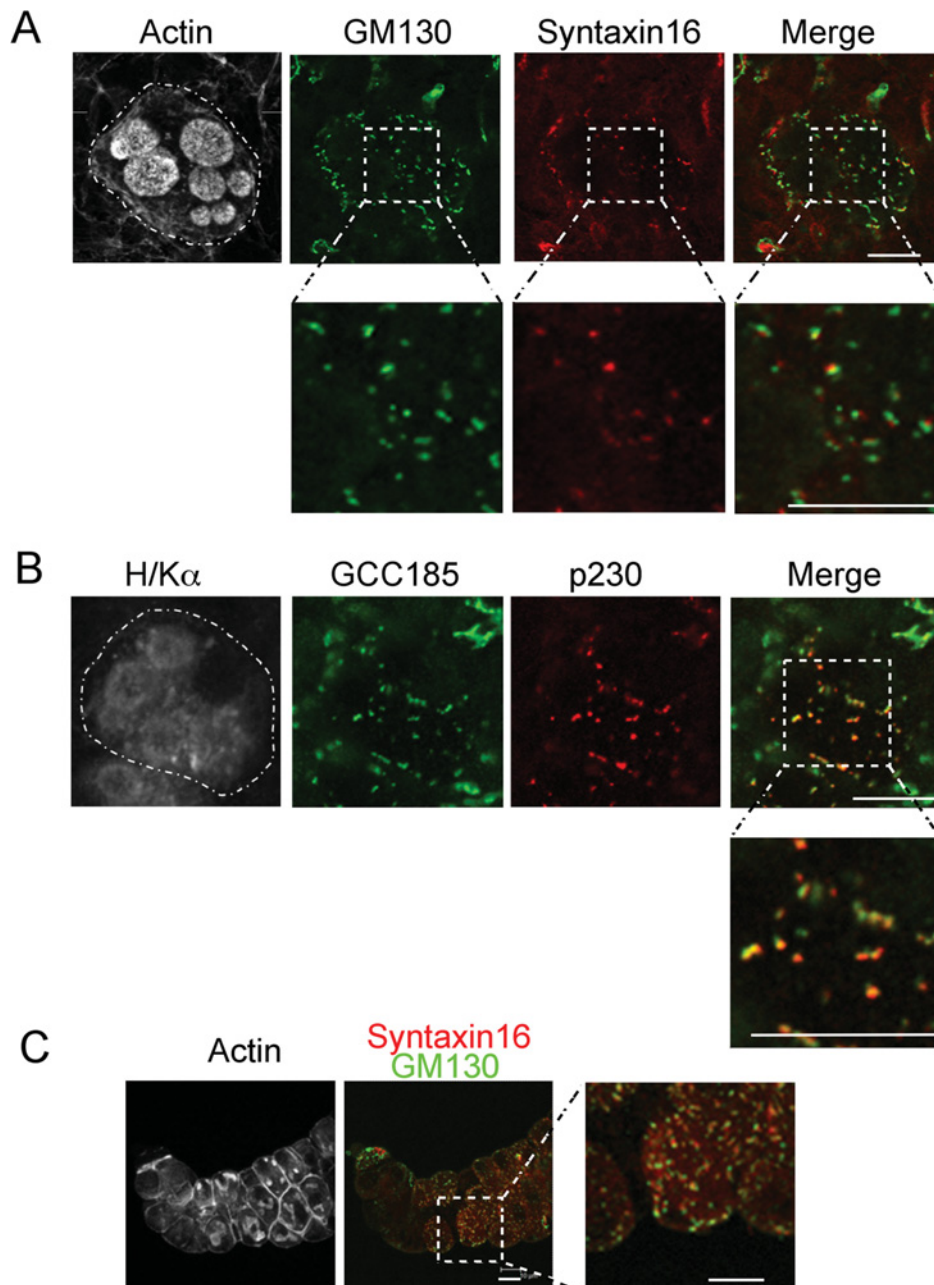
structures of the parietal cells represent intact Golgi stacks.

Following these observations, we wished to establish whether the Golgi apparatus was present as isolated membrane fragments in both resting and active mouse parietal cells. Two populations of gastric cells were obtained: one cultured in the presence of the $H_2$-receptor antagonist, ranitidine, to assure that the cells were in the resting state, whereas the second population of cells was stimulated with histamine, an $H_2$-receptor agonist. Stimulation was carried out in the presence of an $H^+,K^+$ ATPase inhibitor, SCH28080, to prevent the expansion of the intracellular SC vacuoles. Parietal cells were identified by the presence of both actin-rich intracellular SC vacuoles and the $H^+,K^+$ ATPase. The majority of the $H^+,K^+$ ATPase resides in the TVE membranes when a parietal cell is in the resting state. The parietal cells cultured in non-stimulating conditions showed very little co-localization between actin and $H^+,K^+$ ATPase staining, as expected (Supplementary Figure S1 available at http://www.biolcell.org/boc/103/boc1030559add.htm). The diffuse, cytoplasmic staining pattern of $H^+,K^+$ ATPase indicates that the $H^+,K^+$ ATPase is present in the cytoplasmic TVE, indicating that this cell was in the resting state, and consistent with what we expected for the localization of the enzyme to the TVE. Parietal cells stimulated by the addition of histamine showed a significant proportion of the $H^+,K^+$ ATPase on actin-rich SC vacuoles, indicating that this cell was in the active state (Supplementary Figure S1). In both resting and activated parietal cells, the TGN marker GCC88 (Golgi coiled-coil protein of 88 kDa) was present on punctate membrane structures dispersed throughout the cytoplasm. Therefore the Golgi shows a dispersed staining pattern in both resting and active parietal cells.

To ensure that the dispersed Golgi pattern observed was not an artefact induced by tissue culture, we examined gastric glands after isolation from the stomach tissue. The presence of actin-rich SC indicated the location of parietal cells within a gland (Figure 2C). The punctuate-staining patterns for GM130 and the TGN marker syntaxin 16 in intact gastric glands were similar to those found using cultured gastric cells, with multiple, dispersed Golgi units observed, and many of the Golgi units co-labelled with GM130 and syntaxin 16 (Figure 2C). These findings indicate that the parietal cells in their normal physiological environment have an atypical Golgi morphology.

## The association between scattered Golgi stacks and microtubules in parietal cells

Given the importance of the microtubular network in defining the location of the Golgi apparatus in mammalian cells, we assessed the relationship between the dispersed Golgi stacks and microtubules in parietal cells. To visualize the microtubules of parietal cells, a cultured gastric cell population was stained for actin, $\alpha$-tubulin and the TGN marker, GCC88. Non-parietal gastric cells showed the typical radial distribution of microtubules (results not shown), whereas parietal cells had microtubules displaying a disorganized non-radial distribution (Figure 3A). Many of the GCC88-labelled Golgi stacks ($\sim$90%) were in close physical proximity to microtubules (Figure 3A), suggestive of a physical link between the dispersed Golgi stacks and the microtubule network of parietal cells. The association between dispersed Golgi stacks and microtubules was observed in all parietal cells viewed ($>$50).

To determine if the Golgi morphology in parietal cells was regulated by the microtubule network, cultured gastric cells were treated with nocodazole to depolymerize microtubules, and stained with antibodies against $H^+,K^+$ ATPase and GCC88. As expected, the juxta-nuclear Golgi of non-parietal gastric cells was fragmented and dispersed by nocodazole treatment (Supplementary Figure S2 available http://www.biolcell.org/boc/103/boc1030559add.htm). On the other hand, the GCC88 staining patterns of untreated parietal cells and cells treated with nocodazole were very similar (Figures 3B and 3C). There did not appear to be a difference between the size of the GCC88-positive Golgi stacks of untreated and nocodazole-treated parietal cells, indicating that the dispersed Golgi stacks of parietal cells do not undergo any further fragmentation following the depolymerization of microtubules.

## GRASP65 (Golgi reassembly stacking protein 65) is localized to the dispersed Golgi stacks

GRASP65 is *cis*-Golgi protein known to play a key role in forming lateral bridges between the individual stacks of the mammalian Golgi ribbon. Depletion of GRASP65 causes fragmentation of the Golgi

**Figure 3 | Relationship between dispersed Golgi stacks and microtubules in parietal cells**

Gastric cells were cultured for 24 h in gland culture medium containing ranitidine and were fixed in 1% formaldehyde, permeabilized and stained with TRITC-conjugated phalloidin, mouse anti-$\alpha$-tubulin antibodies followed by FITC-conjugated to anti-mouse IgG and (**A**) rabbit anti-GCC88 antibodies followed by Alexa Fluor® 647-conjugated to anti-rabbit IgG. (**B**, **C**) Gastric cells were cultured for 24 h in gland culture medium containing ranitidine, equilibrated in serum-free medium for 1 h, then either (**B**) fixed directly or (**C**) incubated in serum-free medium containing nocodazole for 1 h at 37°C (no $CO_2$). Cells were fixed in 1% formaldehyde, permeabilized and stained with mouse anti-HK$\alpha$ antibodies followed by FITC-conjugated to anti-mouse IgG and rabbit anti-GCC88 antibodies followed by Alexa Fluor® 568-conjugated to anti-rabbit IgG. Scale bars represent 10 $\mu$m.
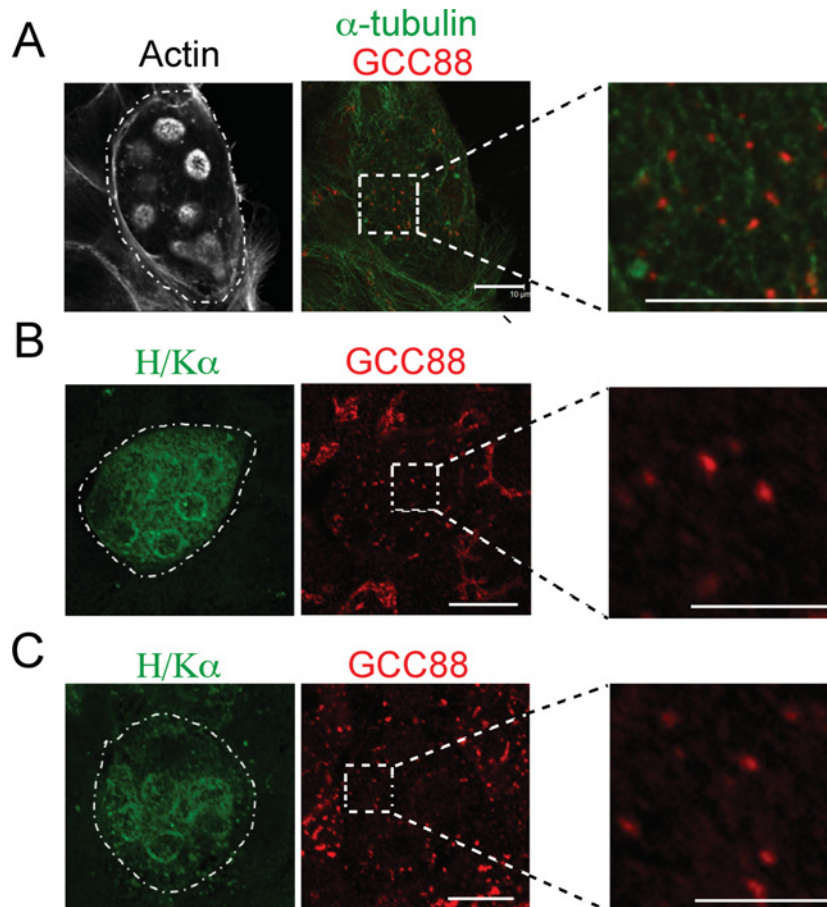


ribbon, and, considering the absence of a Golgi ribbon in the mouse parietal cells, we determined if these cells express GRASP65. Cultured gastric cells were stained for actin, GRASP65 and GM130 (Supplementary Figure S3 available at http://www.biolcell.org/boc/103/boc1030559add.htm). All of the Golgi stacks that stained for GM130 also stained for GRASP65 and there was almost complete overlap between these Golgi components. This result indicates that GRASP65 is localized to the *cis*-Golgi of the dispersed Golgi stacks.

## The dispersed Golgi stacks of parietal cells function in anterograde and retrograde membrane transport

To determine whether the dispersed Golgi stacks in parietal cells were functional, we examined their ability to receive cargo by the anterograde or retrograde membrane transport pathways. The dispersed distribution of Golgi stacks in parietal cells also provides the opportunity to assess whether there may be functional heterogeneity in the population of Golgi mini-stacks, as is the case for the Golgi stacks in

*Drosophila* imaginal disc cells (Yano et al., 2005). First, we assessed the steady-state distribution of the cargo TGN38, a protein that cycles between the plasma membrane and the Golgi apparatus of mammalian cells (Lieu and Gleeson, 2010), and which has been widely used as a model cargo in mammalian cells. If the Golgi stacks are functional in membrane transport then we would expect TGN38 to localize to the dispersed Golgi stacks of parietal cells under steady-state conditions. To induce *de novo* expression of TGN38 in differentiated parietal cells, cultured gastric cells were transduced with a recombinant adenovirus encoding the rat *TGN38* gene. Transduced cells were cultured for 48 h and stained with antibodies against actin, to define the parietal cells, and against GCC185 and TGN38. In transduced nonparietal cells, TGN38 was localized, as expected, predominantly in the perinuclear fashion typical of the Golgi apparatus (Figure 4A). In transduced parietal cells, TGN38 was located on both the cell surface and on punctate fragments scattered throughout the cytoplasm (Figure 4B). The TGN38 punctate cytoplasmic structures showed significant co-localization with GCC185 (Figure 4B). Quantification revealed that 98% of the GCC185 fragments co-localized with or were physically adjacent to TGN38-labelled fragments. These findings demonstrate that the dispersed Golgi stacks are functional and can process cargo for anterograde transport to the cell surface.

Retrograde transport pathways transporting cargo from the plasma membrane to the Golgi have been identified (Johannes and Popoff, 2008; Lieu and Gleeson, 2011); these pathways involve the selective transport of cargo from endosomes to the juxtanuclear-localized Golgi apparatus. Given the dispersed Golgi fragments in parietal cells, the question arises whether there is a functional plasma membrane-to-Golgi retrograde pathway in parietal cells. Therefore we examined the trafficking of the model cargo ChTxB (cholera toxin B) that can undergo retrograde transport to the Golgi in other cells. Cultured parietal cells were incubated with fluorescently tagged ChTxB for 45 min on ice, after which cells were incubated at 37°C to induce internalization of the surface-bound ChTxB–GM₁ complex. Cells were fixed at various time-points to track internalization of the toxin, and then stained for GM130 to mark the Golgi stacks. At the 0 min time-point, the staining pattern for ChTxB indicated that the toxin was bound to the surface of the parietal cell (Figure 4C). Following 90 min of incubation at 37°C, ChTxB was detected both on the cell surface and on punctate structures scattered throughout the cytoplasm (Figure 4C). Some of the punctate ChTxB fragments also co-stained for GM130. A similar finding was also observed using the TGN marker GCC88 (results not shown). Quantification of Golgi-localized ChTxB revealed that approx. 25% of total ChTxB co-localized with the GM130 marker after 4 h of internalization (Figure 5A). In addition, the percentage of GM130-marked Golgi stacks that co-stained for the cargo increased from ~30% after 1 h of internalization to ~50% after 4 h of internalization (Figure 5B). Together, these results show that the plasma membrane-to-Golgi transport pathway is functional in parietal cells and that the majority of Golgi mini-stacks can receive cargo via retrograde transport.

## Parietal cells from mutant mice, HK$\beta^{-/-}$ and Y20A, have dispersed Golgi stacks

A unique feature of parietal cells is the very abundant TVE membranes in the apical cytoplasm. To investigate whether the presence of this extensive cytoplasmic membrane system was directly responsible for promoting the reorganization of the Golgi apparatus in these differentiated cells, we exploited genetically modified mouse lines with the parietal cells lacking specialized TVE. Mice deficient in the H$^+$,K$^+$ ATPase $\beta$-subunit (HK$\beta$) do not have a functional gastric H$^+$,K$^+$ ATPase, are unable to secrete gastric acid and show prominent morphological changes in their parietal cells, including a dramatic reduction in the size of the TVE (Scarff et al., 1999). Cultured gastric cells from the stomachs of HK$\beta^{-/-}$ mice were stained for H$^+$,K$^+$ ATPase $\alpha$-subunit (HK$\alpha$) to identify parietal cells, and the TGN marker GCC185. GCC185 was located on multiple isolated structures scattered throughout the cytoplasm of the cell (Figure 6A), similar to the Golgi staining pattern described for wild-type parietal cells.

Parietal cells were also examined from a second mouse line that express the H$^+$,K$^+$ ATPase with a mutation in the YXX$\varphi$ motif of the cytoplasmic tail of HK$\beta$ (Y20A). In contrast to the HK$\beta$-deficient mice, H$^+$,K$^+$ ATPase activity is expressed in the parietal cells of the Y20A mice, but it is located on the SC regardless of the activation state of the cell. Y20A

**Figure 4 | Transport of model cargo to Golgi stacks in cultured parietal cells**

(**A**, **B**) Steady-state localization of TGN38 in transduced parietal cells. Cultured gastric cells were transduced with TGN38 adenovirus, cultured for 48 h, equilibrated in serum-free medium for 1 h and fixed in 1% formaldehyde, permeabilized and stained with TRITC-conjugated phalloidin, rabbit anti-GCC88 or anti-GCC185 antibodies followed by Alexa Fluor® 647-conjugated to anti-rabbit IgG and mouse anti-TGN38 antibodies followed by FITC-conjugated to anti-mouse IgG. (**A**) Non-parietal gastric cell and (**B**) parietal cell. (**C**) Internalization of ChTxB in cultured parietal cells. Gastric cell populations were cultured for 24 h in gland culture medium containing ranitidine, cells were equilibrated in serum-free medium for 1 h, then incubated with FITC-conjugated ChTxB fragment (2.5 $\mu$g/ml) for 45 min on ice in the presence of SCH28080. Cells were washed and then either fixed directly (0 min) or incubated in serum-free medium containing SCH28080 for 90 min at 37°C (no $CO_2$). Cells were fixed in 1% formaldehyde, permeabilized and stained with TRITC-conjugated phalloidin and anti-mouse GM130 (*cis*-Golgi marker) antibodies followed by Alexa Fluor® 647-conjugated to anti-mouse IgG. Scale bars represent 10 $\mu$m.
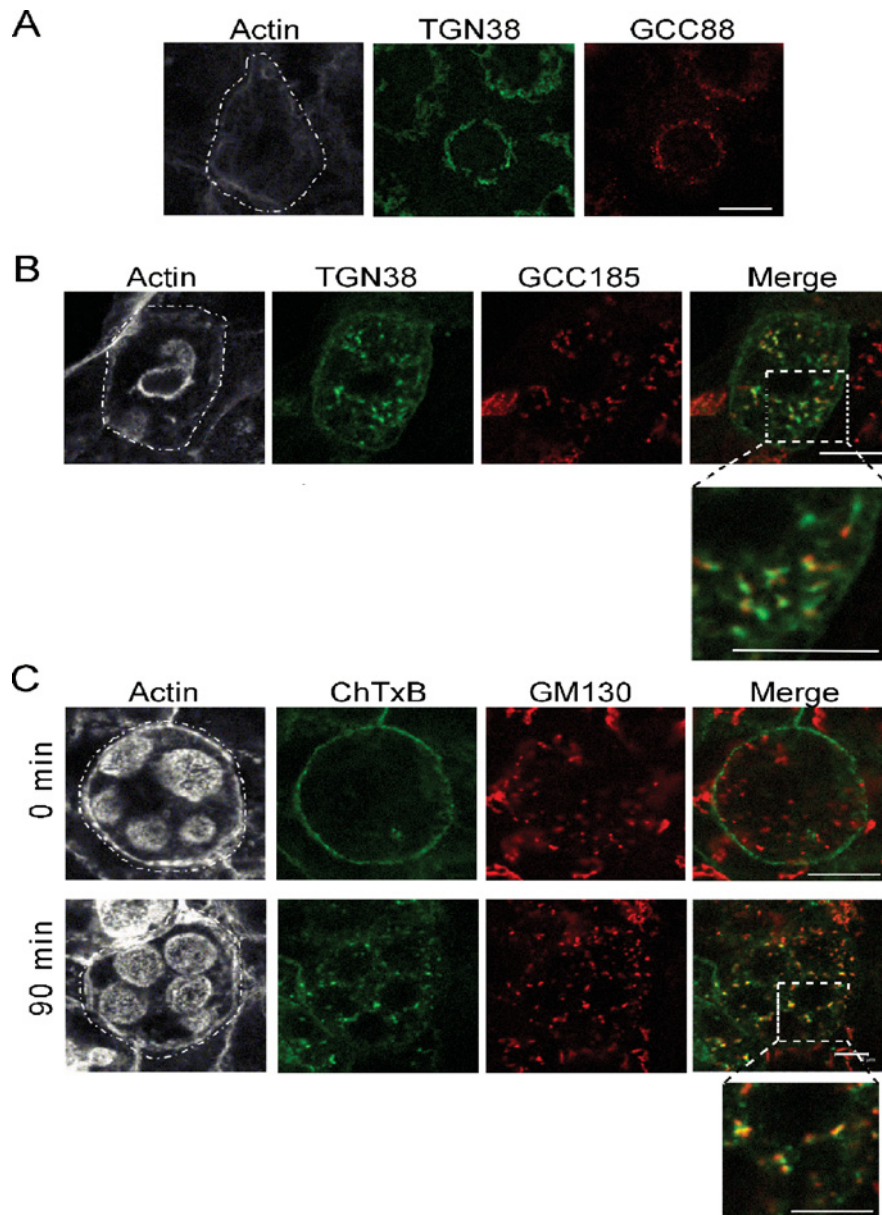
Cultured gastric cells were incubated with FITC–ChTxB on ice, as described in the legend for Figure 4, and then the surface-bound ChTxB was allowed to internalize over a 4 h period. At the indicated time points cells were fixed and permeabilized, and stained for actin and either GCC88 or GM130. (**A**) The number of ChTxB pixels that overlapped with Golgi markers was expressed as a percentage of the total number of ChTxB pixels within each cell using Metamorph software ($n = 10$ for each time-point) as described in Materials and methods section. In (**B**) the number of Golgi structures that co-localized with internalized ChTxB is shown.
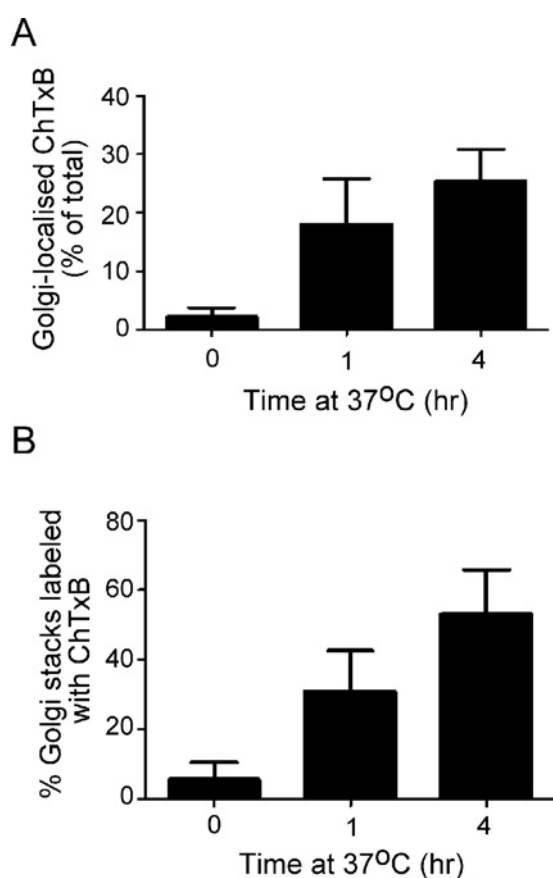


mice can secrete acid, but show prominent morphological changes in their parietal cells, including the complete absence of the TVE. Cultured gastric cells from these mice were stained for actin, GM130 and the TGN marker p230. GM130 and p230 stain was observed in punctate fragments scattered throughout the cytoplasm of the parietal cell (Figure 6B).

The majority of GM130-labelled Golgi units (111 of 121: 91.7%) co-localized with, or were physically adjacent to, p230-labelled units, indicating the presence of dispersed Golgi mini-stacks. These results show that two different mutant mice, $HK\beta^{-/-}$ and Y20A, which have gross morphological changes in their parietal cells, all had the Golgi morphology observed in wild-type parietal cells. Hence, the presence of the TVE is not a controlling factor in the reorganization of the Golgi apparatus.

## Discussion

Parietal cells are polarized epithelial cells solely responsible for the acidification of the lumen of the stomach. These highly specialized cells within the gastric gland undergo a staggering amount of membrane cycling in order to strictly control pH in the stomach. EM studies had previously revealed that the Golgi apparatus is very abundant in newly differentiated parietal cells, but appeared poorly developed in mature parietal cells (Hayward, 1967; Forte et al., 1969; Ito, 1987). By analysing the staining patterns of markers of the *cis*- and *trans*-membrane regions of the Golgi, and 3D (three-dimensional) reconstructions of the labelled Golgi, here we have demonstrated that the Golgi of parietal cells is not present as a ribbon of membrane in the juxta-nuclear region, but it is present as individual Golgi stacks which are scattered throughout the cytoplasm. The Golgi stacks of parietal cells are able to process newly synthesized cargo, and can receive cargo that has undergone retrograde transport. This is a very unusual organization of the Golgi apparatus in a post-mitotic mammalian cell and is likely to reflect the spatial features of the endomembrane system in this differentiated cell type.

The Golgi membrane structures detected throughout the cytoplasm of parietal cells are likely to represent individual Golgi stacks as each structure was found to contain both *cis*- and *trans*-markers, and 3D reconstructions demonstrated that the structures were distinct entities and there was no change in the size of the Golgi structures following nocodazole treatment. The Golgi structures were observed not only in cultured parietal cells but also in parietal cells within intact gastric glands, confirming that the Golgi is present as dispersed structures within the normal physiological environment. On the other

**Figure 6 | The parietal cells of HK$\beta^{-/-}$ and Y20A mice show dispersed Golgi stacks**
Gastric cell populations were isolated from the stomachs of (**A**) HK$\beta^{-/-}$ and (**B**) Y20A mice (fasted) and cultured for 24 h in gland culture medium. Cultured gastric cells were fixed in 1% formaldehyde, permeabilized and stained with (**A**) mouse anti-HK$\alpha$ antibodies followed by FITC-conjugated anti-mouse IgG, and rabbit anti-GCC185 antibodies followed by Alexa Fluor® 568-conjugated to anti-rabbit IgG, and (**B**) TRITC-conjugated phalloidin, mouse anti-GM130 antibodies followed by FITC-conjugated anti-mouse IgG, and human anti-p230 antibodies followed by Alexa Fluor® 647-conjugated to anti-human IgG. Scale bars represent 10 $\mu$m.
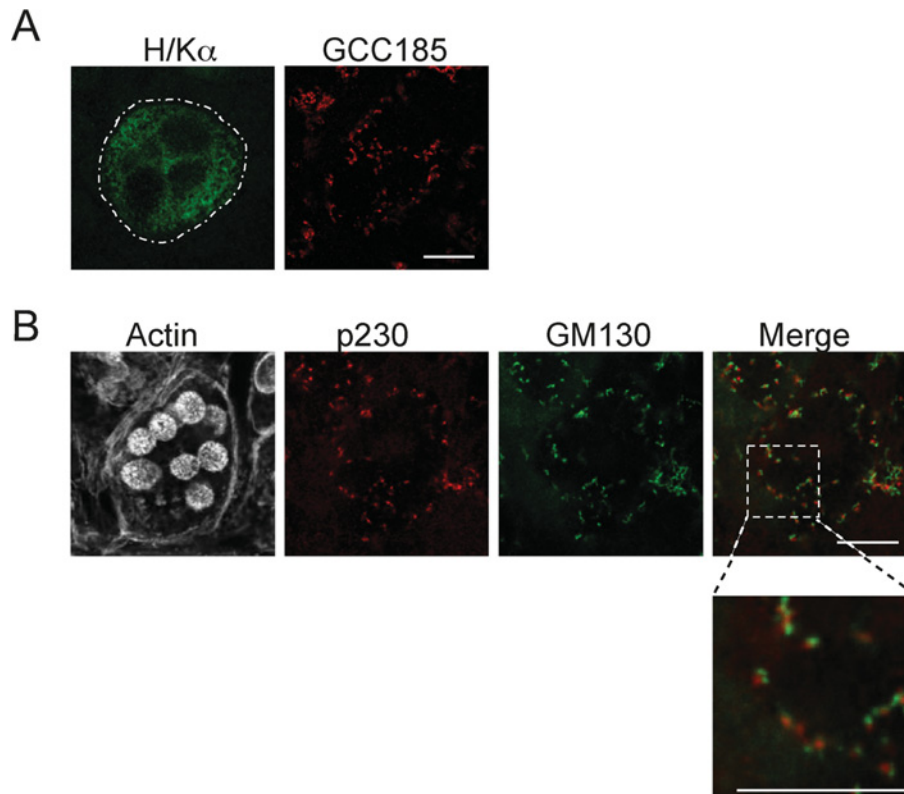


hand, the Golgi of other cells of the gastric gland were organized in a more typical ribbon structure close to the nucleus, highlighting the unique features of the Golgi in specialized acid-secreting cells of the gastric glands. These findings are consistent with electron micrographs of mature parietal cells that have detected intact single Golgi stacks, but rarely multiple stacks in the same section (Ito, 1987; Sawaguchi et al., 2002). Fragmented Golgi were observed in both resting and activated parietal cells, parietal cells that had lost the ability to secrete acid (HK$\beta^{-/-}$) and parietal cells that are devoid of TVE (Y20A). Hence, the distribution of dispersed Golgi stacks throughout the cytoplasm of mature parietal cells is a permanent feature of this cell type and does

not represent a transient reorganization of the Golgi ribbon, as occurs, for example, during mitosis. A fragmented Golgi also provides an explanation for why this organelle has been considered to be small and inconspicuous in parietal cells.

The dispersed Golgi stacks of cultured parietal cells were shown to function in membrane transport and process the model cargos TGN38 and ChTxB. These findings demonstrated that the scattered Golgi stacks of cultured parietal cells were functional components of regulated membrane transport in both the biosynthetic and endocytosis pathway. Indeed, this is the first demonstration of a functional retrograde endosome-to-TGN transport pathway in the gastric parietal cell. As the bulk of ChTxB was found

associated with internalized endosomes and Golgi, rather than TVE membranes, this finding shows that the transport pathways within the endomembrane-rich parietal cell maintain are very selective and that transport to the TVE is likely to require a distinct transport pathway.

Microtubules play a key role in defining the structure and localization of the Golgi in mammalian cells during interphase. Golgi-derived microtubules that are regulated by CLASPs draw Golgi stacks together in a tangential fashion and are critical for the formation of a continuous ribbon (Efimov et al., 2007; Miller et al., 2009). In non-polarized cells, Golgi membrane interacts with microtubules of the radial centrosomal array and the ribbon is positioned near the centrosome via this interaction (Rios and Borens, 2003). Microtubules in a radial centrosomal array were observed in cultured gastric cells (non-parietal) stained with antibodies against $\alpha$-tubulin. In these cells, the Golgi was located in a region where microtubule ends accumulated, close to the nucleus, which is the location of the MTOC. In contrast the $\alpha$-tubulin staining pattern of cultured parietal cells showed microtubules in a relatively disorganized array. The scattered Golgi stacks were in close physical proximity to microtubules in the cytoplasm of parietal cells, suggesting that there may be an association between the stacks and microtubules. The microtubule array of polarized epithelial cells is often aligned along the apical–basal axis (Li and Gundersen, 2008); nonetheless, the Golgi typically forms a ribbon-like convoluted structure located in the apical region (Bacallao et al., 1989). Therefore the presence of individual Golgi stacks in mature epithelial cells is most unusual.

The Golgi apparatus deviates from a ribbon conformation in a variety of situations. Plant cells do not have a ribbon structure; rather, the Golgi consists of large number of individual Golgi stacks (Faso et al., 2009; Hawes et al., 2010). In yeast cells, the Golgi has been identified as either ordered individual stacks, as in *Pichia pastoris,* or individual cisternae spread throughout the cytoplasm (Papanikou and Glick, 2009). *Drosophila* imaginal disc cells have dispersed Golgi mini-stacks (Yano et al., 2005). Interestingly, these cells have two distinct populations of Golgi mini-stacks: one that process basolaterally destined cargo and another that process apically destined cargo (Yano et al., 2005). Such an arrangement does

not appear to be the case with the scattered Golgi stacks of parietal cells as no distinction between the stacks could be identified, as the majority of stacks were shown to be positive for TGN38 or receive ChTxB from the cell surface. Isolated Golgi stacks have been reported in a few specialized mammalian cells, for example, in oocytes and skeletal muscle cells (Lu et al., 2001; Moreno et al., 2002). Recently, Golgi fragmentation was also shown to occur during differentiation of uroepithelial cells of the urinary bladder, a process considered to be important to promote the delivery of components to form the specialized apical membrane of the blood–urine barrier (Kreft et al., 2010). Hence, the reorganization of the Golgi to promote specialized apical membranes and functions is common feature of uroepithelial cells and parietal cells. It is interesting to consider whether the dispersed Golgi stacks observed in parietal cells may result from a mechanism similar to the regulated fragmentation observed in cellular processes. During both mitosis and apoptosis Golgi fragmentation occurs following the modification of GRASP65, a protein that physically links adjacent Golgi stacks (Lane et al., 2002; Rabouille and Kondylis, 2007). However, the fragmented Golgi structure in parietal cells is not due to the down-regulation of GRASP65, as GRASP65 is located on the dispersed Golgi stacks. However, it is possible that GRASP65 is post-translationally modified in parietal cells.

In summary, this work has revealed that gastric parietal cells have a Golgi that does not conform to the ribbon model. Instead, they have numerous individual stacks of Golgi scattered throughout the cytoplasm that can function in the synthesis of exogenous protein and retrograde transport. Why would the Golgi be organized in this unusual fashion in parietal cells? One possibility is that the organization of the Golgi reflects the unusual regulated membrane transport pathways of this cell. The scattered Golgi stacks, rather than a juxta-nuclear Golgi ribbon, may provide a more efficient organization for delivery of transport carriers traversing a cytoplasm highly enriched in endosomes of the TVE system. The fragmentation of the Golgi ribbon is likely to be a regulated event during the differential of parietal cells. Understanding the molecular events associated with Golgi fragmentation in parietal cells is likely to provide further insight into the dynamics and biogenesis of this organelle.

# Materials and methods

### Plasmids, antibodies and reagents

For adenovirus generation, pBHGLOX (dE1, E3), the genomic plasmid, and pDC315, the shuttle vector, both required for adenovirus generation, were obtained from Microbix Biosystems (Toronto, Canada). TGN38–CFP (cyan fluorescent protein), a fusion of full-length TGN38 cDNA to the N-terminus of CFP in the pECFP-N1 vector, was kindly provided by Dr Derek Toomre, Yale University (Keller et al., 2001). TGN38 was PCR-amplified from TGN38–CFP using the primers 5′ TGN38 (CGCGAATTCATGCG-GTTCCAGGTTGCGTTG) and 3′ TGN38 (CCGCGTCGACT-CAAAGCTTTAGGTTCAAACGTTG). The resulting PCR product was digested with EcoRI and SalI, and subcloned into pDC315.

The 1H9 mouse mAb (monoclonal antibody) specific for H/K$\alpha$ has been described (Mori et al., 1989). Rabbit polyclonal antibodies against human GCC88 and GCC185 have been previously described (Luke et al., 2003). Mouse mAbs against GM130 and TGN38 were purchased from BD Biosciences (v) (NSW, Australia). A rabbit polyclonal antibody against syntaxin 16 was purchased from Synaptic Systems (Gottingen, Germany). Human autoantibodies against p230 have been previously described (Kooy et al., 1992; Mu et al., 1995). The mouse mAb to $\alpha$-tubulin (DM1A) was from Sigma–Aldrich. Nuclei of cells were detected by incubation with DAPI (4′,6-diamindino-2-phenylindole; Sigma–Aldrich). Actin was detected by incubation with FITC- or TRITC (tetramethylrhodamine $\beta$-idothiocyanate)-labelled phalloidin (Sigma–Aldrich).

Secondary antibodies used for immunofluorescence were sheep anti-mouse IgG-FITC (from Chemicon, Melbourne, Australia) whereas goat anti-mouse IgG-Alexa Fluor® 647, goat anti-rabbit IgG-Alexa Fluor® 568, goat anti-rabbit IgG-Alexa Fluor® 647, goat anti-human IgG-Alexa Fluor® 647 and goat anti-human IgG-Alexa Fluor® 594 were from Molecular Probes (Invitrogen, Carlsbad, CA, U.S.A.).

### Mammalian cell lines

Adenovirus-packaging 293 cells (Microbix Biosystems, Toronto, Canada) were maintained as a semi-confluent monolayer in DMEM (Dulbecco's modified Eagle's medium) supplemented with 10% (v/v) FCS (fetal calf serum), 2 mM L-glutamine, 100 units/$\mu$l penicillin and 0.1% (w/v) streptomycin.

### Isolation of mouse gastric glands and mouse gastric epithelial cell cultures

Mice were housed under conventional conditions at the Bio21 Molecular Science and Biotechnology animal facility. All experiments were performed with the approval of the University of Melbourne Ethics Committee (ethics number: 0809107). Wild-type mice were BALB/c CrSlc. HK$\beta^{-/-}$ mice (Scarff et al., 1999) and Atp4b-Y20A mice (Nguyen et al., 2004) were on a BALB/c background.

Gastric glands were isolated from stomachs of 2- to 3-month-old mice as described by Gliddon et al. (2008). Briefly, mice were fasted overnight and killed by $CO_2$ asphyxiation. The abdominal and chest cavity were cut open and warm oxygenated perfusion PBS (1 mM $MgSO_4$, 1 mM $CaCl_2$ and dissolved in PBS) was perfused into the left ventricle. The exsanguinated

stomach was quickly excised and the antrum and forestomach removed using a scalpel blade. The stomach was cut along the lesser curvature, turned inside out exposing the rugae, rinsed in perfusion PBS and placed in a conical flask containing 15 ml of warm, oxygenated isolation medium [DMEM (Gibco BRL), 20 mM Hepes buffer (pH 7.4) and 0.2% BSA; 15 ml/mouse]. The stomach was then digested with 1 mg/ml freshly prepare collagenase type IA (Sigma–Aldrich), dissolved in PBS for 1 h with shaking at 37°C. Using forceps, the partially digested stomach was vigorously shaken from side to side to remove intact gastric glands from the stomach lining. The preparation was then transferred into a 50 ml blue-cap tube and the tissue allowed to sediment for ∼15–20 min and then the supernatant removed. The glands were resuspended in 5 ml of gland medium [DMEM/F12, 1:1 (Sigma–Aldrich), pH 7.4, 1% gentamicin, 1% penicillin–streptomycin and 0.5 mM DTT (dithiothreitol; Sigma–Aldrich)], passed through a 100 $\mu$m filter mesh into a clean tube, allowed to settle by gravity, then washed twice in gland medium and re-suspended in 4–5 ml of gland culture medium.

For cell cultures, mouse gastric glands were washed once in gland culture medium [DMEM/F12, pH 7.4, 0.2% BSA (Sigma), 1% gentamicin, 100 ng/ml EGF (epidermal growth factor; Sigma), 5 ng/ml ITSS (Sigma–Aldrich) and 4 ng/ml hydrocortisone (Sigma–Aldrich)] and resuspended in 8 ml gland culture medium. In some cases, 100 $\mu$M ranitidine:HCl was added to the gland culture medium. The glands were slowly pipetted on to coverslips that had been coated with Matrigel basement membrane matrix (BD Biosciences), and cultured in a humidified incubator in air at 37°C.

### Activation of cultured mouse parietal cells

Gastric glands were isolated from mouse stomachs and cultured as above. After 24 h in culture, the gland culture medium was removed and the gastric cell cultures incubated with 500 $\mu$l of warm DMEM/F12, pH 7.4, free of antibiotics for at least 2 h. The medium was removed and parietal cells stimulated by incubation of cultures with 500 $\mu$l of DMEM/F12 containing 100 $\mu$M histamine and 30 $\mu$M IBMX (3-isobutyl-1-methylxanthine) for 30 min incubation at 37°C (no $CO_2$). In some cases, 5 $\mu$M SCH28080 or omeprazole was added to the medium to inhibit acid secretion by the gastric $H^+,K^+$ ATPase.

### Nocodazole treatment of cultured cells

Cultured gastric cells were washed twice with serum-free medium, and incubated in DMEM/F12, pH 7.4, containing 20 $\mu$M nocodazole, for 1 h at 37°C, then processed for immunofluorescence microscopy.

### Indirect immunofluorescence

Gastric cells were cultured for at least 72 h then fixed in 1% formaldehyde in PBS or 4% PFA (paraformaldehyde) in PBS, for 15 min at room temperature (20°C), washed in PBS, and permeabilized with 0.5% Triton X-100 in PBS or 0.1% Triton X-100, in PBS for 4 min at room temperature. Monolayers were then blocked by treatment with 2% BSA/PBS for 15 min at room temperature and incubated with primary antibody, diluted in 2% BSA in PBS, for 1 h at room temperature. The cells were washed three times with PBS, and incubated with

secondary antibody, diluted in 2% BSA in PBS, for 30 min at room temperature. Finally, monolayers were washed twice with PBS, and either incubated with a different set of primary and secondary antibodies, or mounted on to microscope slides in Mowiol 4-88 mounting medium. Cells were imaged by confocal microscopy using a Leica TCS SP2 imaging system. For multicolour labelling, images were collected sequentially. $z$-Series were captured sequentially with a Leica TCS SP2 confocal microscope (HCX PL APO, ×100/1.40–0.70 oil objective) and $z$-axis step of 0.244 $\mu$m; 8-bit images were saved at 512×512. $z$-Series were re-constructed using Volocity imaging software.

For analysis of gastric glands, gland preparations were fixed in 4% (v/v) PFA in PBS at room temperature for 20 min, with regular re-suspension of the glands. After fixation, the glands were pelleted by centrifugation for 3 min, 115 $g$ 16°C, washed in PBS and processed as described above. Fixed and permeabilized gastric glands were layered on to coverslips coated with Cell-Tak (BD Biosciences), and stained as for the cell cultures.

### ChTxB subunit internalization assay using cultured parietal cells

Cultured gastric cells were incubated in serum-free medium for 1–2 h at 37°C, then transferred to 4°C for 10 min and washed once with cold DMEM/F12, 1:1, pH 7.4. FITC-labelled ChTxB was incubated with cultured parietal cells in the presence of 5 $\mu$M SCH28080 for 45 min at 4°C. Unbound ChTxB–FITC was removed and monolayers were either fixed immediately, or incubated at 37°C for the indicated time period to track internalization of ChTxB–FITC. After the incubation, monolayers were fixed in cold 1% formaldehyde in PBS for 15 min, permeabilized and stained as described above.

### Transduction of cultured parietal cells with TGN38 recombinant adenovirus

Recombinant adenovirus encoding TGN38 under the control of the CMV (cytomegalovirus) promoter (rAdv-TGN38) was generated by co-transfecting adenovirus-packaging HEK-293 (human embryonic kidney) cells with transgene-encoding shuttle plasmid and AdMax adenovirus genomic plasmid (Microbix Biosystems). Recombinant virus was isolated as plaques in agarose over HEK-293 cell monolayers, amplified in HEK-293 cells and purified by centrifugation, re-suspended in PBS with 10% glycerol and stored at −70°C, as previously described (Londrigan et al., 2010).

For transduction, the recombinant adenovirus was incubated with ViroMag (Oz Biosciences) magnetic nanoparticles for 10 min at room temperature and the resultant mixture added to parietal cell cultures 4–6 h after plating and a magnetic force was applied for 45 min (Gliddon et al., 2008). The cells were cultured as described above. The following day the medium was replaced and cells analysed 24–48 h after transduction.

### Metamorph analysis of images

Confocal images were analysed using Metamorph imaging software. Images were thresholded and the number of ChTxB pixels that overlapped with Golgi markers was expressed as a percentage of the total number of ChTxB pixels within each cell.

### Statistical analysis

Fluorescent data from metamorph analysis were expressed as means ± S.D. and analysed by an unpaired two-tailed Student's $t$ test. $P < 0.05$ was considered as significant.

## Author contribution

Paul Gleeson and Ian van Driel conceived the project and interpreted the data. Priscilla Gunn designed the experiments, analysed the data and wrote the manuscript. Briony Gliddon provided expertise for gastric gland isolation and parietal cell culture. Sarah Londrigan and Andrew Lew helped with generation of the recombinant adenovirus.

## References

Bacallao, R., Antony, C., Dotti, C., Karsenti, E., Stelzer, E.H. and Simons, K. (1989) The subcellular organization of Madin–Darby canine kidney cells during the formation of a polarized epithelium. J. Cell Biol. **109**, 2817–2832

Chia, P.Z. and Gleeson, P.A. (2011) The regulation of endosome-to-Golgi retrograde transport by tethers and scaffolds. Traffic **12**, 939–947

Colanzi, A., Suetterlin, C. and Malhotra, V. (2003) Cell-cycle-specific Golgi fragmentation: how and why? Curr. Opin. Cell Biol. **15**, 462–467

De Matteis, M.A., Mironov, A.A. and Beznoussenko, G.V. (2008)

Efimov, A., Kharitonov, A., Efimova, N., Loncarek, J., Miller, P.M., Andreyeva, N., Gleeson, P., Galjart, N., Maia, A.R., McLeod, I.X. et al. (2007) Asymmetric CLASP-dependent nucleation of noncentrosomal microtubules at the *trans*-Golgi network. Dev. Cell **12**, 917–930

Faso, C., Boulaflous, A. and Brandizzi, F. (2009) The plant Golgi apparatus: last 10 years of answered and open questions. FEBS Lett. **583**, 3752–3757

Forte, J.G. and Zhu, L. (2010) Apical recycling of the gastric parietal cell H,K-ATPase. Annu. Rev. Physiol. **72**, 273–296

Forte, G.M., Limlomwongse, L. and Forte, J.G. (1969) The development of intracellular membranes concomitant with the appearance of HCl secretion in oxyntic cells of the metamorphosing bullfrog tadpole. J. Cell Sci. **4**, 709–727

Forte, J.G., Machen, T.E. and Forte, J.G. (1977) Ultrastructural changes in oxyntic cells associated with secretory function: a membrane re-cycling hypothesis. Gastroenterology **73**, 941–955

Geibel, J.P. and Wagner, C. (2006) An update on acid secretion. Rev. Physiol. Biochem. Pharmacol. **156**, 45–60

Gliddon, B.L., Nguyen, N.V., Gunn, P.A., Gleeson, P.A. and van Driel, I.R. (2008) Isolation, culture and adenoviral transduction of parietal cells from mouse gastric mucosa. Biomed. Mater. **3**, 034117

Hawes, C., Schoberer, J., Hummel, E. and Osterrieder, A. (2010) Biogenesis of the plant Golgi apparatus. Biochem. Soc. Trans. **38**, 761–767

Hayward, A.F. (1967) The ultrastructure of developing gastric parietal cells in the foetal rabbit. J. Anat. **101**, 12

Heuer, D., Rejman Lipinski, A., Machuy, N., Karlas, A., Wehrens, A., Siedler, F., Brinkmann, V. and Meyer, T.F. (2009) *Chlamydia* causes fragmentation of the Golgi compartment to ensure reproduction. Nature **457**, 731–735

Ito, S. (1987) Functional Gastric Morphology. Raven Press, New York

Johannes, L. and Popoff, V. (2008) Tracing the retrograde route in protein trafficking. Cell **135**, 1175–1187

Keller, P., Toomre, D., Diaz, E., White, J. and Simons, K. (2001) Multicolour imaging of post-Golgi sorting and trafficking in live cells. Nat. Cell Biol. **3**, 140–149

Kooy, J., Toh, B.H., Pettitt, J.M., Erlich, R. and Gleeson, P.A. (1992) Human autoantibodies as reagents to conserved Golgi components: characterization of a peripheral, 230-kDa compartment-specific Golgi protein. J. Biol. Chem. **267**, 20255–20263

Kreft, M.E., Di Giandomenico, D., Beznoussenko, G.V., Resnik, N., Mironov, A.A. and Jezernik, K. (2010) Golgi apparatus fragmentation as a mechanism responsible for uniform delivery of uroplakins to the apical plasma membrane of uroepithelial cells. Biol. Cell **102**, 593–607

Kupfer, A., Dennert, G. and Singer, S.J. (1983) Polarization of the Golgi apparatus and the microtubule-organizing center within cloned natural killer cells bound to their targets. Proc. Natl. Acad. Sci. U.S.A. **80**, 7224–7228

Lane, J.D., Lucocq, J., Pryde, J., Barr, F.A., Woodman, P.G., Allan, V.J. and Lowe, M. (2002) Caspase-mediated cleavage of the stacking protein GRASP65 is required for Golgi fragmentation during apoptosis. J. Cell Biol. **156**, 495–509

Li, R. and Gundersen, G.G. (2008) Beyond polymer polarity: how the cytoskeleton builds a polarized cell. Nat. Rev. Mol. Cell Biol. **9**, 860–873

Lieu, Z.Z. and Gleeson, P.A. (2010) Identification of different itineraries and retromer components for endosome-to-Golgi transport of TGN38 and Shiga toxin. Eur. J. Cell Biol. **89**, 379–393

Lieu, Z.Z. and Gleeson, P.A. (2011) Endosome-to-Golgi transport pathways in physiological processes. Histol. Histopathol. **26**, 395–408

Londrigan, S.L., Sutherland, R.M., Brady, J.L., Carrington, E.M., Cowan, P.J., d'Apice, A.J., O'Connell, P.J., Zhan, Y. and Lew, A.M. (2010) *In situ* protection against islet allograft rejection by CTLA4Ig transduction. Transplantation **90**, 951–957

Lu, Z., Joseph, D., Bugnard, E., Zaal, K.J. and Ralston, E. (2001) Golgi complex reorganization during muscle differentiation: visualization in living cells and mechanism. Mol. Biol. Cell **12**, 795–808

Luke, M.R., Kjer-Nielsen, L., Brown, D.L., Stow, J.L. and Gleeson, P.A. (2003) GRIP domain-mediated targeting of two new coiled-coil proteins, GCC88 and GCC185, to subcompartments of the trans-Golgi network. J. Biol. Chem. **278**, 4216–4226

Miller, P.M., Folkmann, A.W., Maia, A.R., Efimova, N., Efimov, A. and Kaverina, I. (2009) Golgi-derived CLASP-dependent microtubules control Golgi organization and polarized trafficking in motile cells. Nat. Cell Biol. **11**, 1069–1080

Moreno, R.D., Schatten, G. and Ramalho-Santos, J. (2002) Golgi apparatus dynamics during mouse oocyte *in vitro* maturation: effect of the membrane trafficking inhibitor brefeldin A. Biol. Reprod. **66**, 1259–1266

Mori, Y., Fukuma, K., Adachi, Y., Shigeta, K., Kannagri, R., Tanaka, H., Sakai, M., Kuribayashi, K., Uchino, H. and Masuda, T.C. (1989) Characterisation of parietal cell autoantigens involved in neonatal thymectomy-induced murine autoimmune gastritis using monoclonal antibodies. Gastroenterology **97**, 364–375

Mu, F.T., Callaghan, J.M., Steele-Mortimer, O., Stenmark, H., Parton, R.G., Campbell, P.L., McCluskey, J., Yeo, J.P., Tock, E.P. and Toh, B.H. (1995) EEA1, an early endosome-associated protein. EEA1 is a conserved alpha-helical peripheral membrane protein flanked by cysteine 'fingers' and contains a calmodulin-binding IQ motif. J. Biol. Chem. **270**, 13503–13511

Nelson, W.J. (2000) W(h)ither the Golgi during mitosis? J. Cell Biol. **149**, 243–248

Nguyen, N.V., Gleeson, P.A., Courtois-Coutry, N., Caplan, M.J. and van Driel, I.R. (2004) Gastric parietal cell acid secretion in mice can be regulated independently of H/K ATPase endocytosis. Gastroenterology **127**, 145–154

Papanikou, E. and Glick, B.S. (2009) The yeast Golgi apparatus: insights and mysteries. FEBS Lett. **583**, 3746–3751

Rabouille, C. and Kondylis, V. (2007) Golgi ribbon unlinking: an organelle-based $G_2/M$ checkpoint. Cell Cycle **6**, 2723–2729

Rios, R.M. and Borens, M. (2003) The Golgi apparatus at the cell centre. Curr. Opin. Cell Biol. **15**, 60–66

Rogalski, A.A., Bergmann, J.E. and Singer, S.J. (1984) Effect of microtubule assembly status on the intracellular processing and surface expression of an integral protein of the plasma membrane. J. Cell Biol. **99**, 1101–1109

Sawaguchi, A., McDonald, K.L., Karvar, S. and Forte, J.G. (2002) A new approach for high-pressure freezing of primary culture cells: the fine structure and stimulation-associated transformation of cultured rabbit gastric parietal cells. J. Microsc. **208**, 158–166

Scarff, K.L., Judd, L.M., Toh, B.H., Gleeson, P.A. and van Driel, I.R. (1999) Gastric $H^+,K^+$-adenosine triphosphatase beta subunit is required for normal function, development, and membrane structure of mouse parietal cells. Gastroenterology **117**, 605–618

Shin, J.M., Munson, K., Vagin, O. and Sachs, G. (2009) The gastric HK-ATPase: structure, function, and inhibition. Pflügers Arch. **457**, 609–622

Short, B., Haas, A. and Barr, F.A. (2005) Golgins and GTPases, giving identity and structure to the Golgi apparatus. Biochim. Biophys. Acta **1744**, 383–395

Thyberg, J. and Moskalewski, S. (1985) Microtubules and the organization of the Golgi complex. Exp. Cell Res. **159**, 1–16

van Driel, I.R. and Callaghan, J.M. (1995) Proton and potassium transport by $H^+/K^+$-ATPases. Clin. Exp. Pharmacol. Physiol. **22**, 952–960

Yadav, S., Puri, S. and Linstedt, A.D. (2009) A primary role for Golgi positioning in directed secretion, cell polarity, and wound healing. Mol. Biol. Cell **20**, 1728–1736

Yano, H., Yamamoto-Hino, M., Abe, M., Kuwahara, R., Haraguchi, S., Kusaka, I., Awano, W., Kinoshita-Toyoda, A., Toyoda, H. and Goto, S. (2005) Distinct functional units of the Golgi complex in *Drosophila* cells. Proc. Natl. Acad. Sci. U.S.A. **102**, 13467–13472

Yao, X. and Forte, J.G. (2003) Cell biology of acid secretion by the parietal cell. Annu. Rev. Physiol. **65**, 103–131

# Supplementary online data

# The Golgi apparatus in the endomembrane-rich gastric parietal cells exist as functional stable mini-stacks dispersed throughout the cytoplasm

**Priscilla A. Gunn\*, Briony L. Gliddon\*[1], Sarah L. Londrigan†[2], Andrew M. Lew†, Ian R. van Driel\* and Paul A. Gleeson\*[3]**

\*Department of Biochemistry and Molecular Biology and Bio21 Molecular Science and Biotechnology Institute, The University of Melbourne, Victoria 3010, Australia, and †The Walter and Eliza Hall Institute of Medical Research, Parkville 3052, Victoria 3010, Australia

**Figure S1 | The Golgi staining pattern in resting and stimulated cultured parietal cells**

Gastric cell populations were isolated from the stomachs of wild-type mice (fasted) and cultured for 24 h in gland culture medium containing ranitidine. Cultured parietal cells were: (**A**) fixed immediately or (**B**) equilibrated in serum-free medium for 1 h, then incubated in serum-free media containing histamine, IBMX (isobutylmethylxanthine) and SCH28080 for 30 min at 37°C. Cells were fixed in 1% formaldehyde, permeabilized and stained with TRITC (tetramethylrhodamine $\beta$-isothiocyanate)-conjugated phalloidin, mouse anti-HK$\alpha$ antibodies followed by FITC-conjugated anti-mouse IgG, and rabbit anti-GCC88 [TGN (trans-Golgi network) marker] antibodies followed by Alexa Fluor® 647-conjugated anti-rabbit IgG. A broken white line denotes the boundary of an individual cell. Scale bars represent 10 $\mu$m.
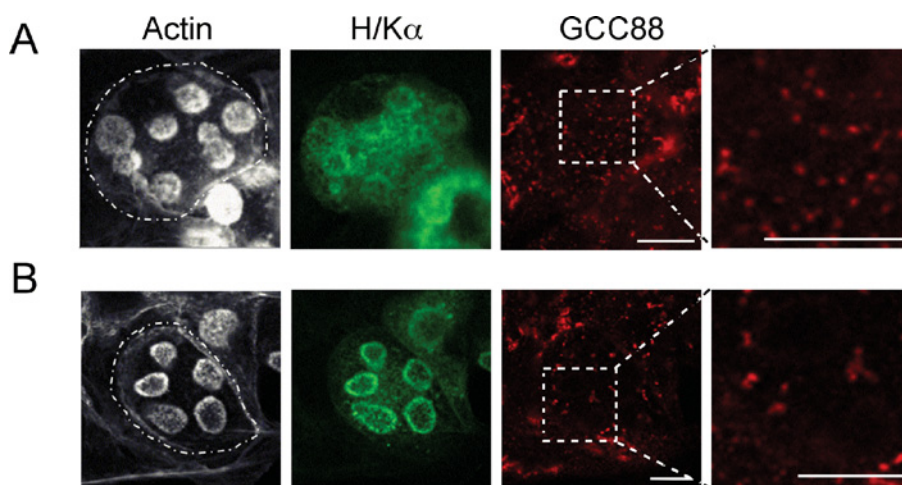
[1]Current address: Centre for Cancer Biology SA Pathology, Adelaide SA 5000, Australia.

[2]Current address: Department Microbiology and Immunology, The University of Melbourne,VIC, Australia.

[3]To whom correspondence should be addressed (email pgleeson@unimelb.edu.au).

**Figure S2 | Nocodazole treatment of cultured gastric cells fragments the Golgi ribbon in non-parietal cells**

Gastric cells were isolated from the stomachs of wild-type mice (fasted) and cultured for 24 h in gland culture medium containing ranitidine. Cells were equilibrated in serum-free medium for 1 h, then either (**A**) fixed directly or (**B**) incubated in serum-free media containing nocodazole for 1 h at 37°C (no $CO_2$). Cells were fixed in 1% formaldehyde, permeabilized and stained with mouse anti-HK$\alpha$ antibodies followed by FITC-conjugated to anti-mouse IgG, rabbit anti-GCC88 antibodies followed by Alexa Fluor® 568-conjugated to anti-rabbit IgG and DAPI (4′,6-diamidino-2-phenylindole). Scale bars represent 10 $\mu$m.

---
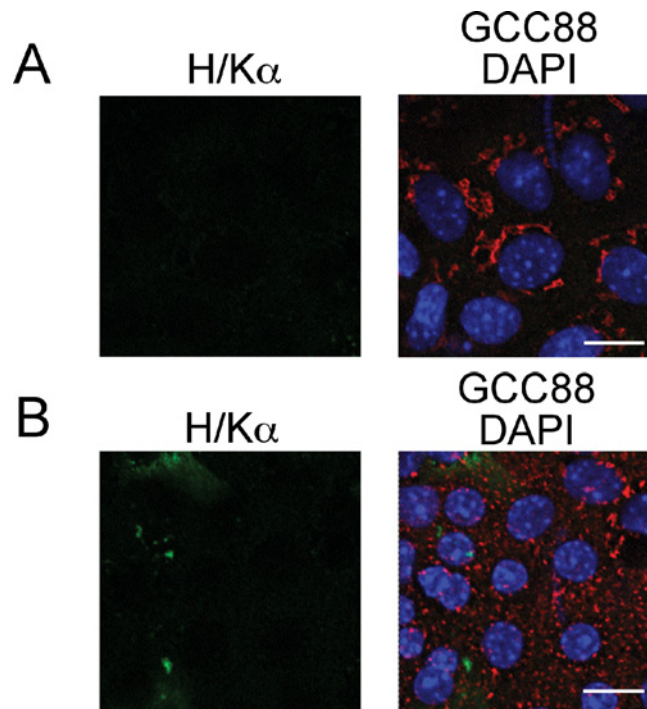
**Figure S3 | GRASP65 (Golgi reassembly stacking protein 65) is located on the dispersed Golgi stacks in parietal cells**

Gastric cell populations were isolated from the stomachs of wild-type mice and cultured for 24 h in gland culture medium containing ranitidine. Cells were fixed in 1% formaldehyde, permeabilized and stained with TRITC-conjugated phalloidin, mouse anti-GM130 antibodies followed by FITC-conjugated to anti-mouse IgG and rabbit anti-GRASP65 antibodies followed by Alexa Fluor® 647-conjugated to anti-rabbit IgG. Scale bars represent 10 $\mu$m.



---

---
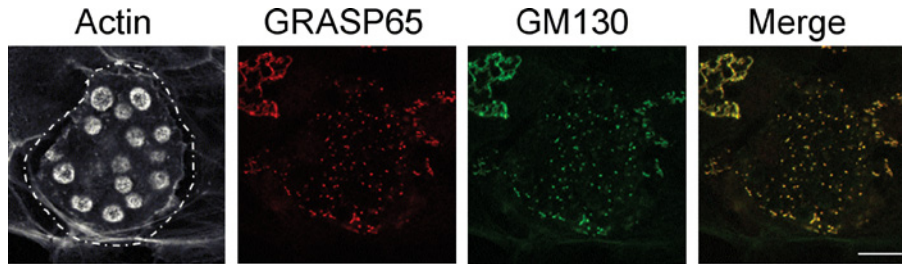
Author/s:

Gunn, PA; Gliddon, BL; Londrigan, SL; Lew, AM; van Driel, IR; Gleeson, PA

Title:

The Golgi apparatus in the endomembrane-rich gastric parietal cells exist as functional stable mini-stacks dispersed throughout the cytoplasm

Date:

2011-12-01